Journal of Innovative Optical Health Sciences
Vol. 5, No. 1 (2012) 1150001 (10 pages)

DOI: 10.1142/S1793545811500015

THE FEASIBILITIES OF USING THE STATISTICAL, FRACTAL AND SINGULAR PROCESSING OF HOMINAL BLOOD PLASMA PHASE IMAGES DURING THE DIAGNOSTICS AND DIFFERENTIATION OF MAMMARY GLAND PATHOLOGICAL STATES

YU. A. USHENKO
Chernivtsi National University
Correlation Optics Department, 2 Kotsyubinsky Str.
Chernivtsi 58012, Ukraine
yuriyu@gmail.com

Accepted 5 July 2011
Published 24 October 2011

Performed in this work are complex statistical, fractal and singular analyses of phase properties inherent to birefringence networks of protein crystals consisting of optically-thin layers prepared from blood plasma. Within the framework of a statistical approach, the authors have investigated values and ranges for changes of statistical moments of the first to the fourth orders that characterize coordinate distributions for phase shifts between orthogonal components of amplitudes inherent to laser radiation transformed by blood plasma with various pathologies. In the framework of the fractal approach, determined are the dimensions of self-similar coordinate phase distributions as well as features of transformation of logarithmic dependences for power spectra of these distributions for various types of hominal mammary gland pathologies.

Keywords: Polarization; birefringence; phase; Jones matrix; blood plasma; statistic moments; fractal; singularity.

1. Introduction

Among the methods for optical diagnostics of human biological tissues (BT), the methods of laser polarimetric diagnostics aimed at their optically anisotropic structure are widely used.[1–30] The main "information product" of these methods is the availability of coordinate distributions for azimuths $\alpha(x, y)$ and ellipticity $\beta(x, y)$ of polarization (polarization maps) with the following types of analyses: statistical (statistical moments of the first to fourth orders[3–5,13,24,29]), correlation (auto- and joint correlation function[11,16–20]), and fractal (fractal dimensionalities[7–9,24,25]). As a result, interrelations between the set of these parameters and distributions of optical axis directions as well as values of the birefringence characterizing the network of optically uniaxial protein (myosin, collagen, elastin, etc.) fibrils in optically anisotropic components of BT layers can be determined. Using this base, a set of methods has been developed for early recognition and differentiation of pathological changes in BT structures related

with their degenerative-dystrophic and oncological changes.[3–5,12,18–20,22–24,28]

In parallel with traditional statistical investigations, the new optical approach has been devised in the recent 10 to 15 years to describe a structure of polarizationally inhomogeneous fields in the case of scattered coherent radiation. The main feature of this approach is the analysis of definite polarization states to determine the whole structure of coordinate distributions for azimuths and ellipticities of polarization. The so-called polarization singularities are commonly used as these states[21,27]:

(1) states with linear polarization when the direction of rotation for the electric field vector is indefinite, the so-called L-points;
(2) circularly polarized states when the azimuth of polarization for the electric field vector is indefinite, the so-called C-points.

It is noteworthy that there exists a widespread group of optically anisotropic biological objects for which the methods of laser polarimetric diagnostics are not so efficient. Optically thin (coefficient of extinction $\tau \leq 0.1$) layers of various biological liquids (such as bile, urine, liquor, synovial liquid and blood plasma) can be related to these objects. All these layers possess considerably less optical anisotropy of the biological component matter as compared with birefringent BT structures.[3,9,13] As a consequence, these objects weakly modulate polarization of laser radiation $\left(\begin{cases} \alpha(x,y) \approx \text{const.} \\ \beta(x,y) \to 0. \end{cases}\right)$. On the other hand, the biological liquids are more available for a direct laboratory analysis as compared to traumatic methods of BT biopsy. From the above reasoning, it seems topical to search new, additional parameters for laser diagnostics of optically anisotropic structures in biological liquids.

Our work is aimed at searching the possibilities to perform diagnostics and differentiation of structures inherent to liquid-crystal networks of blood plasma with various pathologies (norm-mastopathy-breast cancer) by using the method to determine the coordinate distributions of phase shifts (phase maps) between orthogonal components of laser radiation amplitudes with the following statistical, fractal and singular analyses of these distributions.

2. Polarization Modeling of Properties Inherent to Networks of Biological Protein Crystals in Blood Plasma

As a base for analyses of processes providing formation of polarization-inhomogeneous images of blood plasma, we use the optical model developed in Refs. 3–6, 14, 15, 22 and 26:

- optical properties of blood plasma are determined as those of a two-component amorphous–crystalline structure;
- crystalline component is an architectonic net consisting of amino acid liquid crystals;
- optically, the amino acid liquid crystals possess the properties of uniaxial birefringent and optically active crystals.

The optical properties of amorphous $\{A\}$ and crystalline $\{C\}$ components of blood plasma can be exhaustively described using the following Jones operators[3]:

$$\{A\} = \left\| \begin{matrix} a_{11} & a_{12} \\ a_{21} & a_{22} \end{matrix} \right\| = \left\| \begin{matrix} \exp(-\tau l) & 0 \\ 0 & \exp(-\tau l) \end{matrix} \right\|; \tag{1}$$

$$\{C\} = \left\| \begin{matrix} c_{11} & c_{12} \\ c_{21} & c_{22} \end{matrix} \right\| = \left\| \begin{matrix} \cos^2\rho + \sin^2\rho \exp(-i\delta) & \cos\rho \sin\rho[1 - \exp(-i\delta)] \\ \cos\rho \sin\rho[1 - \exp(-i\delta)] & \sin^2\rho + \cos^2\rho \exp(-i\delta) \end{matrix} \right\| \times \left\| \begin{matrix} \cos\theta & \sin\theta \\ -\sin\theta & \cos\theta \end{matrix} \right\|. \tag{2}$$

Here, τ is the absorption coefficient for laser radiation in the blood plasma layer with the geometric thickness l; ρ — direction of the optical axis; $\delta = 2\pi/\lambda \Delta n d$ — phase shift (linear phase anisotropy) between the orthogonal components E_x and E_y of the amplitude of illuminating laser light with the wavelength λ; Δn — index of birefringence; θ — circular phase anisotropy or optical activity index.

The Jones matrix of the blood plasma layer, where isotropic and anisotropic creations lie in one plane, can be expressed as a sum of operators $\{A\}$ and $\{C\}$

$$\{M\} = \{A\} + \{C\} = \left\| \begin{matrix} a_{11} + c_{11} & a_{12} + c_{12} \\ a_{21} + c_{21} & a_{22} + c_{22} \end{matrix} \right\|, \tag{3}$$

Let us consider the process of transformation of the complex amplitude ($E \to U$) of a laser wave that passed through the blood plasma layer ($\{M\}$) located between two crossed phase filters — quarter-wave plates ($\{\Phi_1\}$ and $\{\Phi_2\}$) and polarizers ($\{P_1\}$ and $\{P_2\}$), planes of transmission for which make $+45^\circ$ and -45° angles with axes of the highest velocity. The amplitude U of the transformed laser beam in this experimental setup can be determined from the following matrix equation

$$U = 0.25\{P_2\}\{\Phi_2\}\{M\}\{\Phi_1\}\{P_1\}E. \tag{4}$$

Here,

$$\begin{cases} E = \begin{pmatrix} E_x \\ E_y \exp(-i\delta_0) \end{pmatrix}; \quad U = \begin{pmatrix} U_x \\ U_y \exp(-i\delta) \end{pmatrix}; \\ \{P_1\} = \begin{Vmatrix} 1 & 1 \\ 1 & 1 \end{Vmatrix}; \quad \{P_2\} = \begin{Vmatrix} 1 & -1 \\ -1 & 1 \end{Vmatrix}; \quad \{\Phi_1\} = \begin{Vmatrix} 1 & 0 \\ 0 & i \end{Vmatrix}; \quad \{\Phi_2\} = \begin{Vmatrix} i & 0 \\ 0 & 1 \end{Vmatrix}. \end{cases} \tag{5}$$

In the special case of a plane-polarized wave $E(E_x = E_y; \delta_0 = 0) = \begin{pmatrix} 1 \\ 1 \end{pmatrix}$, Eq. (4) acquires the form

$$U = 0.25 \begin{Vmatrix} 1 & -1 \\ -1 & 1 \end{Vmatrix} \begin{Vmatrix} i & 0 \\ 0 & 1 \end{Vmatrix} \times \begin{Vmatrix} \cos^2\rho + \sin^2\rho \exp[-i\delta] & \cos\rho \sin\rho\{1 - \exp[-i\delta]\} \\ \cos\rho \sin\rho\{1 - \exp[-i\delta]\} & \sin^2\rho + \cos^2\rho \exp[-i\delta] \end{Vmatrix} \times \begin{Vmatrix} 1 & 0 \\ 0 & i \end{Vmatrix} \begin{Vmatrix} 1 & 1 \\ 1 & 1 \end{Vmatrix} \begin{pmatrix} 1 \\ 1 \end{pmatrix}. \tag{6}$$

The solution of the matrix equation (6) is the value of complex amplitude $U(\delta)$ that is determined exclusively by the phase shift δ and does not depend on orientation of the optical axis ρ for a laser image of blood plasma. Based on it, one can write

$$I_\delta(r) = UU^* = I_0 \sin^2\left[\frac{\delta(r)}{2}\right]. \tag{7}$$

Here, I_0 is the intensity of a probing laser beam and $I_\delta(r)$ is intensity of the laser image for the biological liquid layer in the point (r).

Inter-relations (4) to (7) define the algorithm for direct experimental measuring the coordinate distribution of phase shifts $\delta(r)$ between orthogonal components of the amplitudes U_x, U_y in the laser image of an optically anisotropic biological liquid layer.

3. Optical Scheme and Method for Experimental Measuring the Phase Maps of Blood Plasma

Shown in Fig. 1 is the optical scheme for phasometry of laser images obtained for blood plasma.[3–5,30]

Illumination was carried out using the parallel beam ($\varnothing = 10^4\,\mu$m) of He–Ne laser 1 ($\lambda = 0.6328$ μm). Using the polarization illuminator (quarter-wave plate 3 and polarizer 4), we formed the beam linearly polarized with the azimuth 45°. The axis of the highest velocity of the quarter-wave plate 5 was oriented at the angle $\Theta = 45^\circ$ relatively to the transmission plane of the polarizer 4. Images of blood plasma layers 6 were projected using the micro-objective 7 into the plane of the light-sensitive area ($m \times n = 800\,\text{pix} \times 600\,\text{pix}$) of a

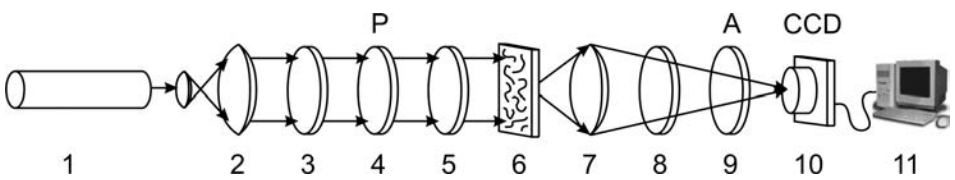

Fig. 1. Optical scheme of the phase meter. 1 — He–Ne laser; 2 — collimator; 3, 5, 8 — quarter-wave plates; 4, 9 — polarizer and analyzer, respectively; 6 — investigated object; 7 — micro-objective; 10 — CCD camera; 11 — personal computer.

CCD camera 10. Rotating the transmission plane of the analyzer 9 by the angle $\Theta = -45^\circ$ relatively to the axis of the highest velocity of the quarter-wave plate 8, formed were the conditions for transmission of left-circular polarized oscillations of points in laser images of blood plasma. The intensity of these oscillations I_δ was registered by each separate pixel in the CCD camera 10. Thus, we obtained the two-dimensional distribution $I_\delta\begin{pmatrix} r_{11}, & r_{1n} \\ r_{m1}, & r_{mn} \end{pmatrix}$ for this intensity. Further, in accordance with (7), we calculated coordinate distributions (phase maps) for phase shifts $\delta(m \times n)$ between orthogonal components of the amplitude for laser images of blood plasma.

4. Algorithms for Statistical and Fractal Analyses of Phase Maps of Blood Plasma Layers

In order to estimate $\delta(m \times n)$ distributions, we have calculated the set of statistic moments $M_{j=1,2,3,4}$

$$M_1 = \frac{1}{N}\sum_{i=1}^{N}|\delta_i|, \quad M_2 = \sqrt{\frac{1}{N}\sum_{i=1}^{N}(\delta_i - M_1)^2},$$
$$M_3 = \frac{1}{Z_2^3}\frac{1}{N}\sum_{i=1}^{N}\delta_i^3, \quad M_4 = \frac{1}{Z_2^4}\frac{1}{N}\sum_{i=1}^{N}\delta_i^4. \tag{8}$$

The fractal analysis of $\delta(m \times n)$ distributions was performed using calculation of logarithmic dependences $\log J(\delta) - \log d^{-1}$ for power spectra $J(\delta)$ using the MatLab software

$$J(\delta) = S(\omega) = \sum_{m=1}^{n} K(m)e^{-j\omega m}, \tag{9}$$

where $K(m)$ is the autocorrelation function of $\delta(m \times n)$ distributions; ω are the normalized frequencies, which correspond to spatial frequencies $(\omega = d^{-1})$ determined by geometrical dimensions (d) inherent to structural elements of laser images for blood plasma.

The dependences $\log J(\delta) - \log d^{-1}$ are approximated using the least-squares method into the curves $V(\eta)$, straight parts of which are used to determine the slope angles η and fractal dimensionalities F in accordance with the relation[3–5]:

$$F = 3 - tg\eta. \tag{10}$$

Classification of coordinate $\delta(m \times n)$ distributions is fulfilled using the following criteria:

- they are fractal with the proviso that the slope angle is constant $(\eta = \text{const.})$ for two to three decades of changing the sizes d;
- they are multi-fractal on the condition that there are available several slope angles $V(\eta)$;
- they are random, if any stable slope angles $V(\eta)$ do not exist within the whole range of changing the sizes d.

In the latter case, the $\log J(\delta) - \log d^{-1}$ distributions are characterized with the dispersion

$$D = \sqrt{\frac{1}{N}\sum_{i=1}^{N}[\log J(\delta) - \log d^{-1}]_i^2}. \tag{11}$$

5. Statistical and Fractal Parameters of Phase Maps of Blood Plasma Layers

As objects for experimental studying, we chose optically thin layers of blood plasma taken from a healthy patient (Fig. 2(a)) and with mastopathy (Fig. 2(b)) and breast cancer (Fig. 2(c)).

The images of layers prepared from blood plasma (Fig. 2) are indicative of availability of two fractions — optically isotropic and liquid-crystal network (anisotropic one). As seen, geometric structure and sizes of separate elements in the polycrystalline network of the samples prepared from blood plasma are individual for physiological state.

Shown in Fig. 3 are the phase maps (fragments (a), (b), (c)) and histograms (fragments (d), (e), (f)) for distributions of random values inherent to the phase shifts δ between orthogonal components of the laser radiation amplitude transformed inside layers of blood plasma in all groups.

The obtained data show that the value of phase shifts δ for laser radiation transformed inside layers of blood plasma lies within the short range of changes $0 \le \delta \le \pi$. The weak phase modulation is related with two factors. First, it is low geometric thickness $(d = 10 \cdots 15\,\mu\text{m})$ of the samples. Second, it is weak birefringence $(\Delta n \sim 10^{-4} \cdots 10^{-2})$ of liquid-crystal structures in blood plasma.

Our comparative analysis of coordinate distributions of random values inherent to phase shifts δ in laser images of both types of blood plasma revealed availability of two dominant extreme

(a) (b) (c)

Fig. 2. Polycrystalline networks of blood plasma of healthy patient (a); with mastopathy (b); and mammary gland cancer of the second stage (c).

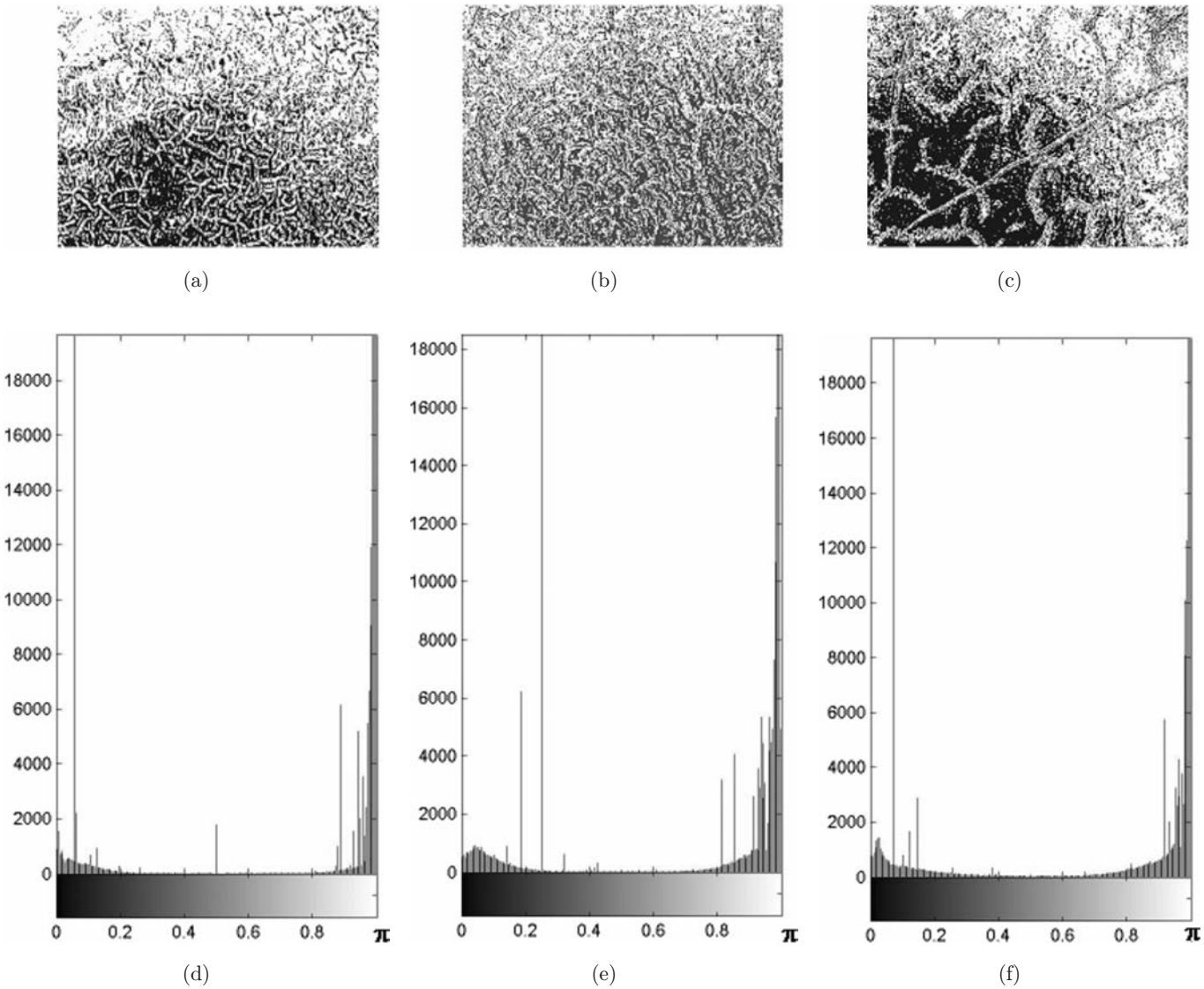

(a) (b) (c)

(d) (e) (f)

Fig. 3. Coordinate (a, b, c) and quantitative (d, e, f) distributions δ of laser images for the samples of blood plasma taken from healthy patient's (a, d); with mastopathy (b, e) and with mammary gland cancer of the second stage (c, f).

Table 1. Statistic moments $M^{\delta}_{i=1-4}$ of the phase coordinate distributions $\delta(x, y)$ of laser radiation, which is transformed by samples of blood plasma of healthy patients and patients affected by mastopathy and mammary gland cancer of the second stage.

$M^{\delta}_{i=1-4}$	Norm (21 patients)	Mastopathy (19 patients)	Cancer (20 patients)
M^{δ}_1	0.28 ± 0.034	0.31 ± 0.036	0.34 ± 0.039
M^{δ}_2	0.32 ± 0.046	0.29 ± 0.034	0.26 ± 0.031
M^{δ}_3	0.73 ± 0.084	0.76 ± 0.079	0.81 ± 0.087
M^{δ}_4	0.46 ± 0.055	0.51 ± 0.062	0.53 ± 0.062

ranges: $0 \le \delta \le 0.15\pi$ and $0.85\pi \le \delta \le \pi$. In our opinion, these features of probabilistic phase distributions are related with the influence of optically isotropic ($\delta \to 0$) and liquid-crystal ($\delta \to \pi$) components in the composition of blood plasma.

Table 1 contains data on the values of statistic moments of the first to fourth order, which characterize the distribution of phase shifts of blood plasma laser images of three groups of healthy ($q = 21$) and affected by mastopathy ($q = 19$) and cancer patients ($q = 20$). The confidence interval for such investigation is the following: $p < 0.01$.

The obtained results show that the differentiation of phase maps of different groups is impossible — change of size and range of statistic moments of first to fourth order almost coincide.

Being aimed at more specific investigation of phase features for both fractions, we used the following method to select information. Such an approach is based on singular analysis of polarization-inhomogeneous images of hominal blood plasma.[5,19,27] From the available coordinate set of values $\delta(m \times n) = \begin{pmatrix} \delta_{11}, \ldots, \delta_{1n} \\ \delta_{n1}, \ldots, \delta_{mn} \end{pmatrix}$ in phase maps (Figs. 3(a) and 3(b)), we found samples of extreme values $\delta(m \times n) = 0$ (linear polarization states — L-points) and $\delta(m \times n) = 0.5\pi$ (circularly polarized states — C-points). In what follows, by scanning along the direction x changes from 1 to n we carried out calculation of the amount of extreme values for phase shifts within the column $m = n \times 1$ pix. Within the limits of each local sample $(1_{\text{pix}} \times n_{\text{pix}}), (k = 1, 2, \ldots, m)$ we computed the amount (N) of extreme values $\delta(k) = 0$ $(N^{(k)}_L)$ and $(N^{(k)}_C)$. Thus, we found the dependences $N_L(x) \equiv (N^{(1)}_L, N^{(2)}_L, \ldots, N^{(m)}_L)i$, $N_C(x) \equiv (N^{(1)}_C, N^{(2)}_C, \ldots, N^{(m)}_C)$ for the amount of extreme values of phase shifts within the limits of laser image for blood plasma.

Figures 4 and 5 show a set of coordinate distributions $\delta(m \times n) = 0; 0.5\pi$ (fragments (a, d, g)) for the dependences of the amount of extreme values $N_{L,C}(x)$ (fragments (b, e, i)) and logarithmic dependences $\log J(N_{L,C}) - \log d^{-1}$ (fragments (c, f, h)) that characterize phase maps for the samples of blood plasma belonging to a healthy patient (fragments (a, b, c)) and a patient with mastopathy (fragments (d, e, f)) and mammary gland cancer of the second stage (fragments (g, l, h)).

The comparative analysis of the obtained set of experimental data about statistical and fractal structures in dependences for the amount of

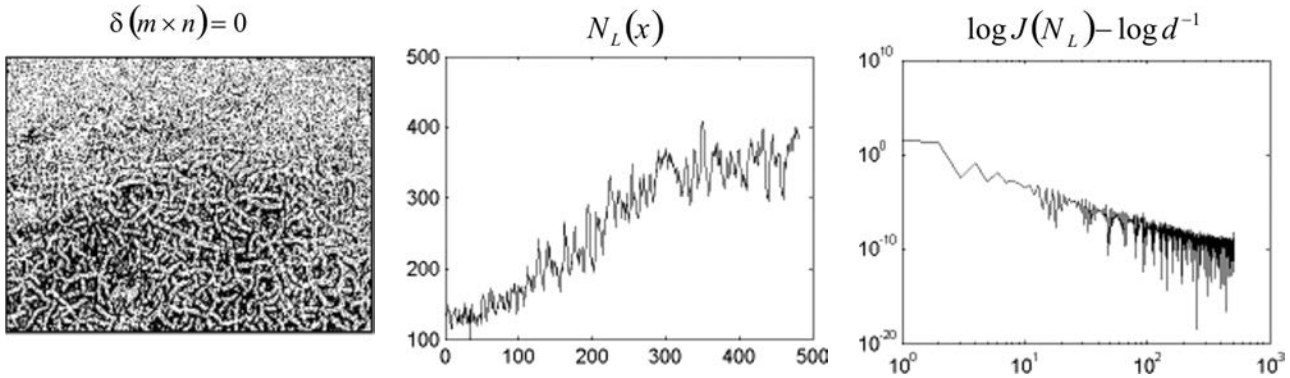

(a) (b) (c)

Fig. 4. Coordinate (a, d, g), quantitative $N_L(x)$ (b, e, l) and fractal $\log J(N_L) - \log d^{-1}$ (c, f, h) parameters of the extreme sample $\delta(m \times n) = 0$ for phase maps of the samples of blood plasma belonging to a healthy patient (a, b, c), patients with mastopathy (d, e, f) and mammary gland cancer of the second stage (g, l, h).

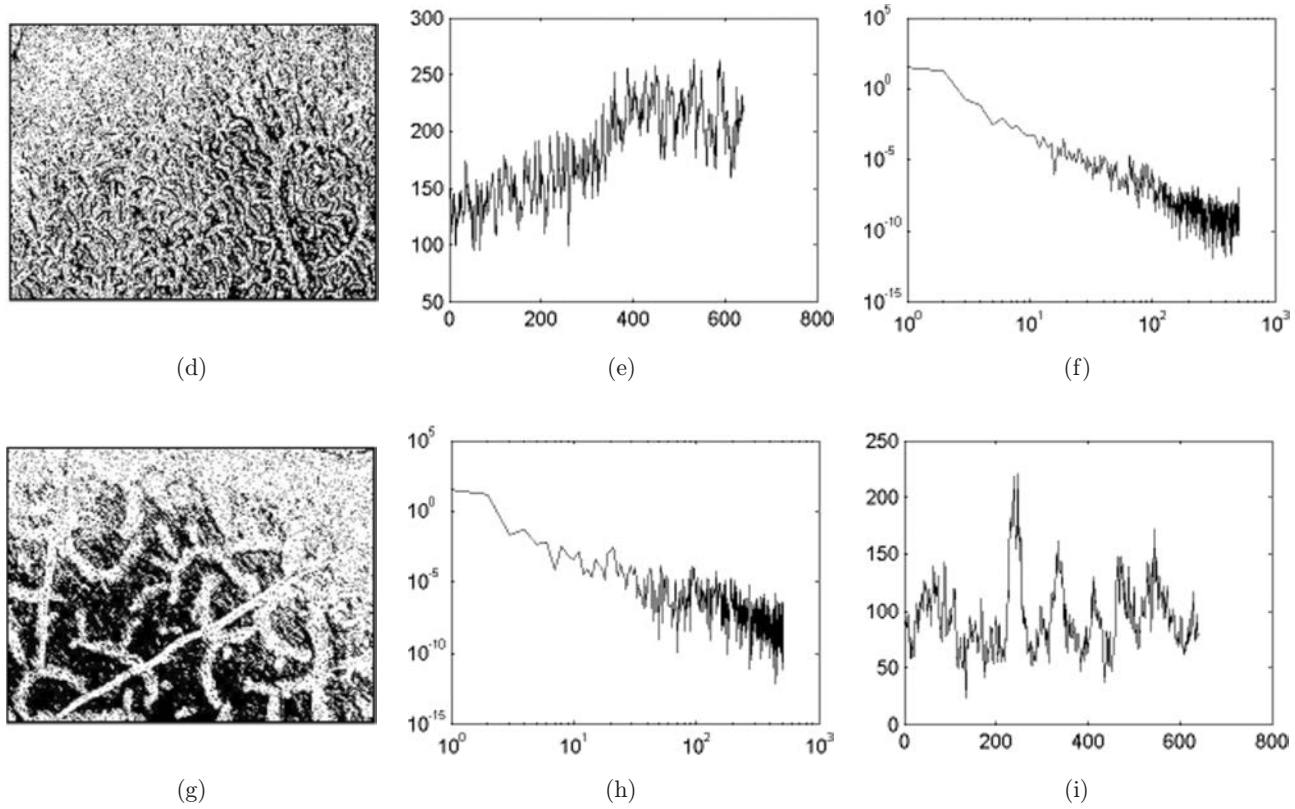

Fig. 4. (*Continued*)

extreme values $N_{L,C}(x)$ inherent to phase maps describing layers of blood plasma in healthy patient and that affected by mastopathy and mammary gland cancer of the second stage enabled to find:

- tendency to a decreasing (increasing) total amount of extreme values $\delta_{\min} \to 0$ ($\delta_{\max} \to 0.5\pi$) of the phase shifts in laser images of layers prepared from blood plasma of a patient with mastopathy and mammary gland cancer of the second stage (Figs. 4 and 5, fragments (b, e, l));
- logarithmic dependences for the power spectra of distributions $N_L(x)$ for the optically isotropic component in blood plasma of all types possess a stable slope angle (Fig. 4, fragments (c, f, h)) within

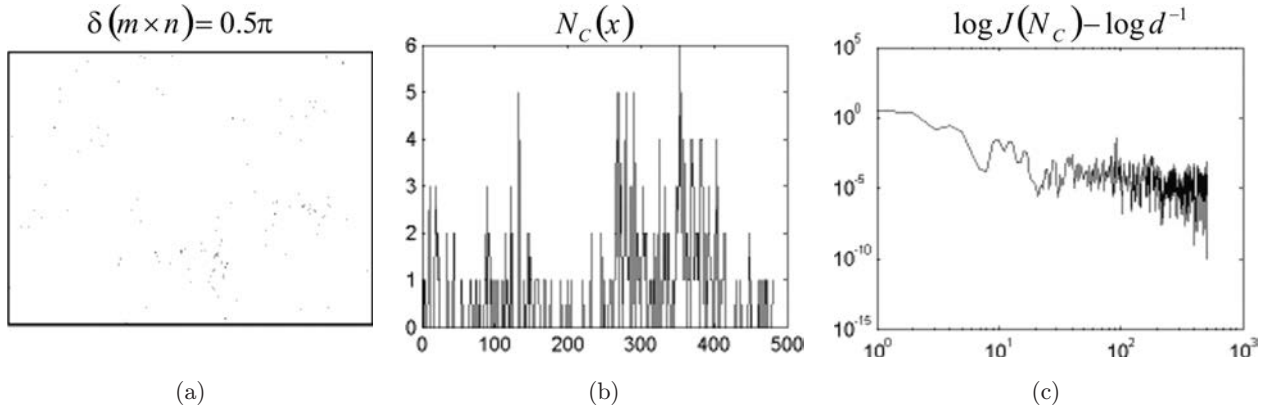

Fig. 5. Coordinate (a, d, g), quantitative $N_C(x)$ (b, e, l) and fractal $\log J(N_C) - \log d^{-1}$ (c, f, h) parameters of the extreme sample $\delta(m \times n) = 0.5\pi$ for phase maps of the samples of blood plasma belonging to a healthy patient (a, b, c), patients with mastopathy (d, e, f) and mammary gland cancer of the second stage (g, l, h).

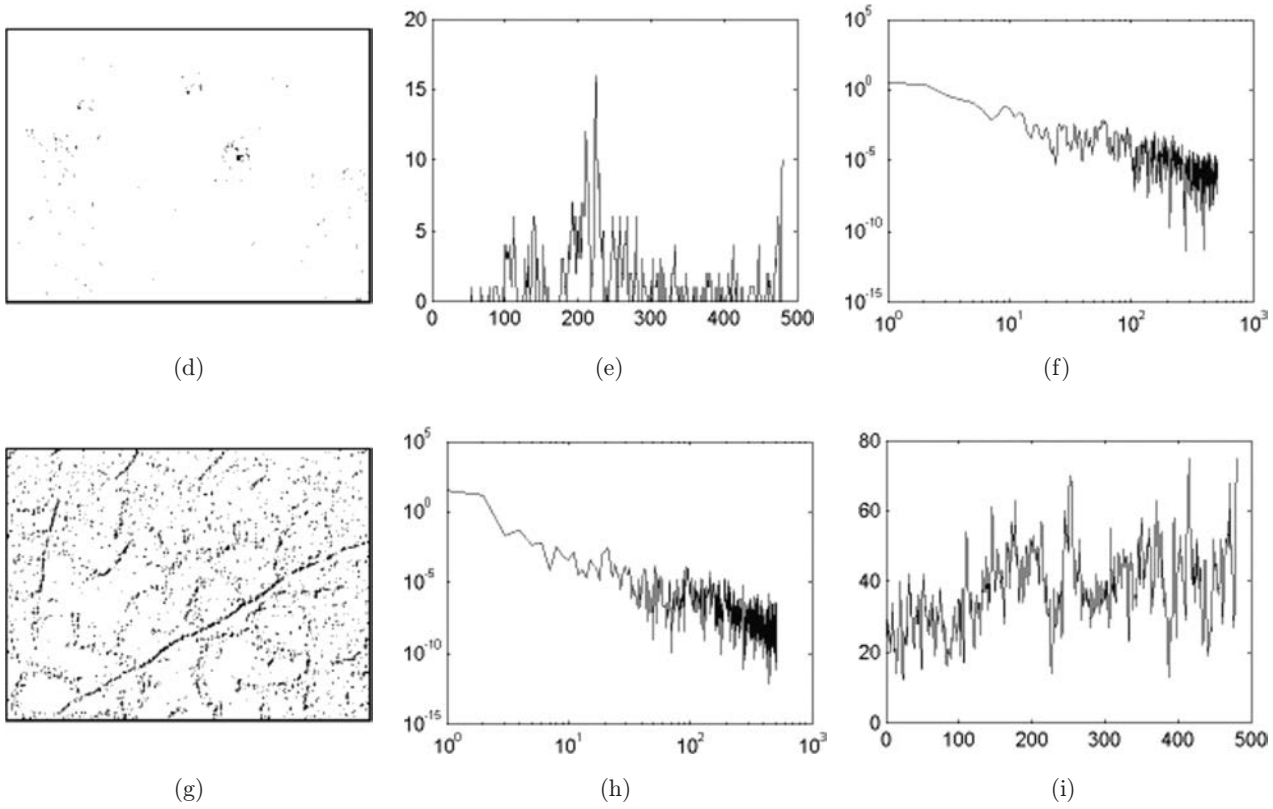

Fig. 5. (*Continued*)

the whole range of geometric sizes inherent to the laser image registered by the CCD camera (Fig. 1);

- statistical distributions $N_C(x)$ for phase maps of laser images describing the optically anisotropic fraction of blood plasma in a healthy man (Fig. 5, fragment (c)) are transformed into the fractal ones in the case of mammary gland cancer of the second stage (Fig. 5, fragment (h)).

From the quantitative viewpoint, the dependences $N_{L,C}(x)$ illustrate statistical $M^{\delta}_{i=1-4}$, and fractal $F^{\delta}; D^{\delta}$ parameters determined within the limits of three patient groups, and they are summarized in Tables 2 and 3.

Our analysis of the parameters determined experimentally has shown that the following parameters are diagnostically sensitive in observation of inflammatory processes

- statistical moments of the third (M^{δ}_3) and fourth (M^{δ}_4) orders in distributions for the amount of extreme values $N_C(x)$ of phase shifts

Table 2. Statistical moments $M^{\delta}_{i=1-4}$ and fractal $F^{\delta}; D^{\delta}$ parameters that characterize the distributions for amounts of extreme values in coordinate distributions $\delta(m \times n) = 0$ of laser images for blood plasma.

$\delta(m \times n) = 0$	Norm (21 patients)	Mastopathy (19 patients)	Cancer (20 patients)
M^{δ}_1	0.51 ± 0.062	0.54 ± 0.063	0.56 ± 0.065
M^{δ}_2	0.16 ± 0.018	0.13 ± 0.015	0.11 ± 0.014
M^{δ}_3	0.22 ± 0.031	0.19 ± 0.025	0.16 ± 0.021
M^{δ}_4	0.46 ± 0.057	0.54 ± 0.066	0.58 ± 0.069
F_1	2.01 ± 0.11	1.94 ± 0.1	1.99 ± 0.14
D^{δ}	0.21 ± 0.029	0.25 ± 0.032	0.29 ± 0.036

Table 3. Statistical moments $M^{\delta}_{i=1-4}$ and fractal $F^{\delta}; D^{\delta}$ parameters that characterize the distributions for amounts of extreme values in coordinate distributions $\delta(m \times n) = 0.5\pi$ of laser images for blood plasma.

$\delta(m \times n) = 0.5\pi$	Norm (21 patients)	Mastopathy (19 patients)	Cancer (20 patients)
M^{δ}_1	0.22 ± 0.025	0.28 ± 0.042	0.33 ± 0.042
M^{δ}_2	0.28 ± 0.031	0.21 ± 0.027	0.14 ± 0.018
M^{δ}_3	0.71 ± 0.088	1.15 ± 0.32	2.07 ± 0.29
M^{δ}_4	0.88 ± 0.099	1,89 ± 0.32	3.12 ± 0.47
F_1	Statistical	2.07 ± 0.14	2.03 ± 0.13
D^{δ}	0.35 ± 0.044	0.29 ± 0.035	0.18 ± 0.022

$\delta(m \times n) = 0.5\pi$ in laser images for blood plasma of healthy patients and affected by mastopathy and cancer of both types — differences between them reach 1.7–2.4 and 2.4–4.1 times, correspondingly;

- distributions $N_C(x)$ for the phase maps describing blood plasma for healthy and sick patients are, respectively, statistical and fractal;
- dispersion D^{δ} of the dependences $\log J(N_C) - \log d^{-1}$ in the case of pathological changes in the polycrystalline structure of blood plasma is 1.75–2.15 times decreased.

6. Conclusions

Thus, one can draw the following conclusions:

(1) Blood plasma, independently of their physiological state, contains phase-modulating optically anisotropic network of biological crystals.
(2) Ascertained and grounded is a set of criteria for phase diagnostics of pathological and cancer processes as being based on statistical (statistical moments of the first to fourth orders) and fractal (fractal dimensionality and dispersion for the distribution of extrema in log–log dependences of power spectra) analyses of phase distributions in laser images of blood plasma.

References

1. W. F. Cheong, S. A. Prahl, A. J. Welch, "A review of the optical properties of biological tissues," *IEEE J. Quantum Electron.* **26**, 2166−2185 (1990).
2. S. A. Prahl, M. Keijzer, S. L. Jacques, A. J. Welch, "A Monte Carlo model of light propagation in tissue," in *SPIE Proceedings of Dosimetry of Laser Radiation in Medicine and Biology*, G. J. Müller, D. H. Sliney, Eds., Vol. IS 5, pp. 102−111 (1989).
3. A. G. Ushenko, V. P. Pishak, "Laser polarimetry of biological tissue: Principles and applications," in *Handbook of Coherent-Domain Optical Methods*: *Biomedical Diagnostics, Environmental and Material Science*, Vol. I, V. V. Tuchin, Ed., Kluwer Academic Publishers, Boston, pp. 93−138 (2004).
4. O. V. Angelsky, A. G. Ushenko, Yu. A. Ushenko, V. P. Pishak, "Statistical and fractal structure of biological tissue Mueller matrix images," in *Optical Correlation Techniques and Applications*, O. V. Angelsky, Ed., Society of Photo-Optical Instrumentation Engineers, Washington, pp. 213−266 (2007).
5. O. V. Angelsky, A. G. Ushenko, Yu. A. Ushenko, V. P. Pishak, A. P. Peresunko, "Statistical, correlation, and topological approaches in diagnostics of the structure and physiological state of birefringent biological tissues," in *Handbook of Photonics for Biomedical Science*, V. V. Tuchin, Ed., CRC Press, USA, pp. 21−67 (2010).
6. A. G. Ushenko, "Polarization structure of laser scattering fields," *Opt. Eng.* **34**, 1088−1093 (1995).
7. A. G. Ushenko, "Laser diagnostics of biofractals," *Quantum Electron* **29**, 1078−1084 (1999).
8. O. V. Angel'skiĭ, A. G. Ushenko, A. D. Arkhelyuk, S. B. Ermolenko, D. N. Burkovets, "Structure of matrices for the transformation of laser radiation by biofractals," *Quantum Electron* **29**, 1074−1077 (1999).
9. O. V. Angel'skiĭ, A. G. Ushenko, A. D. Arkhelyuk, S. B. Ermolenko, D. N. Burkovets, "Scattering of laser radiation by multifractal biological structures," *Opt. Spectrosc.* **88**, 444−448 (2000).
10. A. G. Ushenko, D. N. Burkovets, Yu. A. Ushenko, "Polarization-phase mapping and reconstruction of biological tissue architectonics during diagnosis of pathological lesions," *Opt. Spectrosc.* **93**, 449−456 (2002).
11. A. G. Ushenko, "Stokes correlometry of biotissues," *Laser Phys.* **10**, 1286−1292 (2000).
12. A. G. Ushenko, "The vector structure of laser biospeckle fields and polarization diagnostics of collagen skin structures," *Laser Phys.* **10**, 1143−1149 (2000).
13. A. G. Ushenko, "Laser polarimetry of polarization-phase statistical moments of the object field of optically anisotropic scattering layers," *Opt. Spectrosc.* **91**, 313−316 (2001).
14. A. G. Ushenko, "Polarization contrast enhancement of images of biological tissues under the conditions of multiple scattering," *Opt. Spectrosc.* **91**, 937−940 (2001).
15. A. G. Ushenko, "Laser probing of biological tissues and the polarization selection of their images," *Opt. Spectrosc.* **91**, 932−936 (2001).
16. A. G. Ushenko, "Correlation processing and wavelet analysis of polarization images of biological tissues," *Opt. Spectrosc.* **91**, 773−778 (2002).
17. A. G. Ushenko, "Polarization correlometry of angular structure in the micro-relief pattern or rough surfaces," *Opt. Spectrosc.* **92**, 227−229 (2002).
18. O. V. Angelsky, A. G. Ushenko, Ye. G. Ushenko, "2D Stokes polarimetry of biospeckle tissues images in pre-clinic diagnostics of their pre-cancer states," *J. Holography Speckle* **2**, 26−33 (2005).
19. O. V. Angelsky, A. G. Ushenko, Ye. G. Ushenko, "Complex degree of mutual polarization of biological tissue coherent images for the diagnostics of their

physiological state," *J. Biomed. Opt.* **10**, 060502 (2005).
20. O. V. Angelsky, A. G. Ushenko, Ye. G. Ushenko, "Investigation of the correlation structure of biological tissue polarization images during the diagnostics of their oncological changes," *Phys. Med. Biol.* **50**, 4811−4822 (2005).
21. O. V. Angelsky, A. G. Ushenko, Ye. G. Ushenko, Y. Y. Tomka, "Polarization singularities of biological tissues images," *J. Biomed. Opt.* **11**, 054030 (2006).
22. O. G. Ushenko, S. G. Guminetsky, A. V. Motrich, "Optical properties of urine, blood plasma and pulmonary condensate of the patients with pulmonary form of tuberculosis," *Photoelectron.* **16**, 133−139 (2007).
23. S. H. Guminetskiy, O. G. Ushenko, I. P. Polyanskiy, A. V. Motrych, F. V. Grynchuk, "The optical method for investigation of the peritonitis progressing process," *Proc. SPIE* **7008**, 700827 (2008).
24. A. Ushenko, S. Yermolenko, A. Prydij, S. Guminetsky, I. Gruia, O. Toma, K. Vladychenko, "Statistical and fractal approaches in laser polarimetry diagnostics of the cancer prostate tissues," *Proc. SPIE* **7008**, 70082C (2008).
25. A. G. Ushenko, A. I. Fediv, Yu. F. Marchuk, "Correlation and fractal structure of Jones matrices of human bile secret," *Proc. SPIE* **7368**, 73681Q (2009).
26. A. G. Ushenko, Y. Y. Tomka, V. I. Istratiy, "Polarization selection of two-dimensional phase-inhomogeneous birefringence images of biotissues," *Proc. SPIE* **7388**, 73881L (2009).
27. A. G. Ushenko, A. I. Fediv, Yu. F. Marchuk, "Singular structure of polarization images of bile secret in diagnostics of human physiological state," *Proc. SPIE* **7368**, 73681S (2009).
28. S. B. Yermolenko, A. G. Ushenko, P. Ivashko, "Spectropolarimetry of cancer change of biotissues," *Proc. SPIE* **7388**, 73881D (2009).
29. A. G. Ushenko, I. Z. Misevich, V. Istratiy, I. Bachyns'ka, A. P. Peresunko, O. K. Numan, T. G. Moiysuk, "Evolution of statistic moments of 2D-distributions of biological liquid crystal net Mueller matrix elements in the process of their birefringent structure changes," *Adv. Opt. Technol.* **2010**, 423145 (2010).
30. O. V. Dubolazov, A. G. Ushenko, V. T. Bachynsky, A. P. Peresunko, O. Ya. Vanchulyak, "On the feasibilities of using the wavelet analysis of Mueller matrix images of biological crystals," *Adv. Opt. Technol.* **2010**, 162832 (2010).